Article Identifier
DOI: 10.22032/dbt.58732
URN: urn:nbn:de:gbv:ilm1-2023isc-055:3

60th ILMENAU SCIENTIFIC COLLOQUIUM
Technische Universität Ilmenau, 4 – 8 September 2023
URN: urn:nbn:de:gbv:ilm1-2023isc:1

EMPIRICAL STUDY ON DED-ARC WELDING QUALITY INSPECTION USING AIRBORNE SOUND ANALYSIS

Jaydeep Chauhan[1], Saichand Gourishetti[1], Maximilian Rohe[2], Martin Sennewald[2], Dr. Jörg Hildebrand[2], Prof. Jean Pierre Bergmann[2]

[1] Fraunhofer IDMT, Ilmenau, Germany
[2] Technische Universität Ilmenau, Group Production Technology, Ilmenau, Germany
jaydeep.chauhan@idmt.fraunhofer.de

ABSTRACT

This study explores the potential of audible range airborne sound emissions from Gas Metal Arc Welding (GMAW) to create an automated classification system using neural networks (NN) for weld seam quality inspection. Irregularities in GMAW process (oil presence, insufficient shielding gas) may lead to porosity imperfections in weld seams. Using Directed Energy Deposition-Arc additive manufacturing, aluminum (Al) and steel wall structures were produced with varying shielding gas flows or applying oil. Acoustic emissions (AE) generated during the welding process were captured using audible to ultrasonic range microphones. Mel spectrograms were computed from the AE data to serve as input to NN during training. The proposed model achieved notable accuracies in classifying both Al weld seams (83% binary, 68% multi-class) and steel welds (82% binary, 58% multi-class). These results demonstrate that employing audible range AE and NN in GMAW monitoring offers a viable method for low-latency monitoring and valuable insights into improving welding quality.

Index Terms - Airborne Sound Analysis, Weld Process Quality Monitoring, GMAW, DED-Arc

1. INTRODUCTION

Metal structure manufacturing encompasses various techniques, including powder bed fusion (PBF) and Directed Energy Deposition (DED). Within DED-Arc, methods like GMAW, tungsten inert gas welding (TIG), and plasma processes are employed in additive manufacturing. These processes involve the gradual buildup of a structure by melting and depositing a wire-shaped filler material [1]. The presented study focuses on DED-arc, specifically using the GMAW process. The GMAW [2], is a widely used welding process that involves melting the edges of metals or their alloys using a concentrated arc, with a wire electrode fed to the arc and melted under a shielding gas jacket. The shielding gas surrounds the liquid melt pool, protecting it from contaminants and preventing oxidation during the welding process. GMAW is known for its precision and ability to weld small and delicate parts, making it widely used in industries such as automotive, aviation, aerospace, precision engineering, medical techniques, electronics, and welding of pipelines and pressure valves [3, 4, 5, 6].

However, despite its advantages, workpieces welded with the GMAW process may suffer common imperfections such as porosity, undercut and excessive spatter, which can negatively impact the quality of the welds. Porosity appears as gas bubbles in the weld metal

and is usually caused by the presence of contaminants such as moisture, oil, rust, and inadequate shielding gas coverage. This imperfection in the GMAW process can have several negative effects such as weakened mechanical strength, decreased durability, reduced productivity, and poor aesthetic appearance of weld joints [7]. The detection and classification of the weld process irregularities causing this kind of imperfection in GMAW are therefore of the utmost importance to ensure the integrity and reliability of the welded components.

Several conventional state-of-the-art non-destructive testing methods, including Visual inspection [8], X-ray radiography [9], Eddy current testing [10], and Ultrasonic testing [11], have been employed for defect detection. The application of these methods is limited due to challenges in implementation in low-latency systems and high costs [12]. AE analysis, on the other hand, offers a non-contact approach and allows for inspecting a larger area compared to Ultrasonic testing. The importance of AE in monitoring the arc welding process has been recognized for a long time. Still, there are limited published studies that explore sound waves as a valuable source of information for monitoring welding operations. The first studies on acoustic waves during the GMAW process were conducted by [13] and [14], who discovered synchronization between sound waves and short-circuiting and identified that sound pressure increases with arc length and welding current. Some of the research has been conducted to assess the suitability of different arc signals for online monitoring in automated welding, aiming to improve productivity, reduce costs, and enhance the reliability of welded components. Rostek [15] utilized computer-aided acoustic pattern recognition to analyze acoustic signals and observed the impact of operational parameters on frequency amplitude and noise spectra characteristics. Arata's [16] measurements highlighted the influence of sound on the molten pool behavior and overall welding process quality. Jožef et al. [17] employed audible sound to evaluate and monitor the welding process, as well as predict its stability and quality. Through experimental analysis, this study reveals two primary mechanisms that generate noise: the first being the impulse-like nature of arc extinction and ignition, while the second involves the arc itself functioning as an ionization sound source. Additionally, Mayer [18] explored the use of acoustic signals for online monitoring in submerged arc welding [17].

AE based fault detection methods provide low-latency fault detection capabilities, prompt identification, and intervention in industrial processes. They are highly sensitive to internal imperfections, capturing acoustic signals within the material, and allowing for the detection of hidden faults at early stages. These methods offer non-destructive testing, ensuring integrity and functionality without invasive procedures, and reducing downtime and maintenance costs. AE based fault detection in welding poses several challenges, such as background noise interference [18, 19], signal distortion due to the welding process, the complexity of distinguishing between normal and faulty sounds, and the need for sophisticated signal processing techniques to extract meaningful information from the recorded AE. Many processes, including DED-Arc, suffer from a scarcity of data suitable for the effective utilization of machine learning techniques. Moreover, limited data availability, lack of diversity in data, imbalanced datasets, and inadequate quality annotations further hinder the development and efficacy of automated quality monitoring systems in industrial environments [20, 21].

In DED-Arc specifically, sample sizes are typically limited due to the time-intensive nature of manufacturing, sample preparation, and testing. Labelling the data is a particularly time-consuming task. Data augmentation presents a valuable approach to augmenting both the size and quality of the training data, offering a means to address these limitations [1]. By applying techniques such as random erasing [22], mixup [23], and SpecAugment [24], the augmented data introduces new variations and increases the diversity of the training samples. This enables the model to learn robust and invariant features, improving its ability to generalize to unseen data and enhancing overall performance, even with limited original training data. Johnson et al. [25] utilized image augmentation techniques (such as grid distortion, random brightness,

random erasing, random rotating) on Industrial Sound Analysis datasets. This showcases the suitability of the suggested image augmentation methods when dealing with audio data.

2. WELDING EXPERIMENTS AND AE MEASUREMENT SETUP

To investigate the potential of AE analysis for DED-arc, an experimental setup needed to be designed for recording a dataset in this domain. An acoustic chamber was built around the process using molleton as an absorber to minimize the influence of environmental sounds. Figure 1 illustrates the configuration of the experimental setup to produce the Al and steel walls.

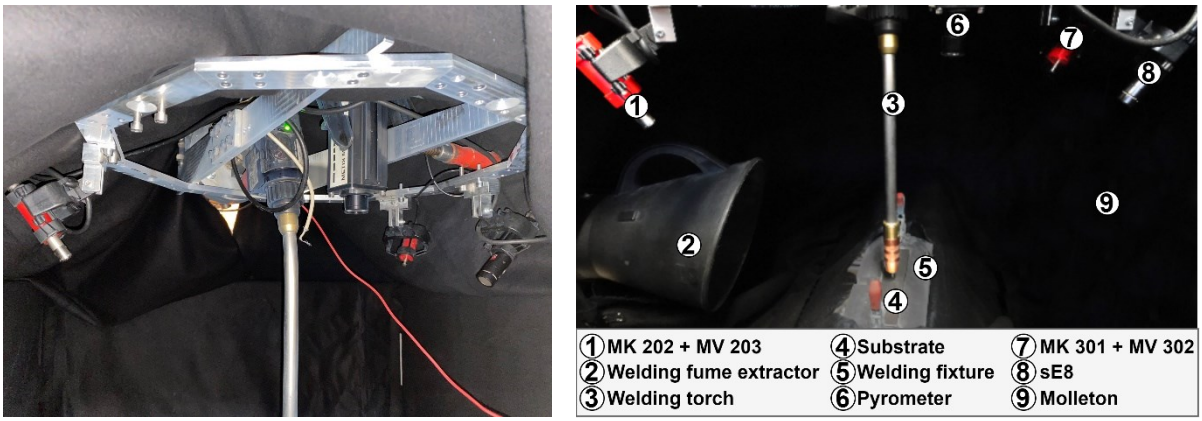

(a) (b)

Figure 1. Experimental setup showing all audio microphones mounted around a metal frame (a) and the named hardware (b) used to record the AE from the Al and steel welds

To ensure a constant sound pressure level, the microphones were mounted on special fixtures (see Figure 1a) with a fixed distance and angle to the arc. During the welding process, the emitted sound is captured in layer by layer using audible range microphones, namely the sE8 and MK202, with a sampling rate of 50 kHz. Additionally, an ultrasonic range microphone (MK301) with a sampling rate of 200 kHz is employed. Dewesoft is used as the data acquisition system for this purpose.

Initially, experiments were conducted using Al weld seams, followed by experimentation with steel. Using a Fronius TPS 500i welding machine and a Kuka KR60 as a handling system, additive-manufactured Al alloy (AlMg4.5) walls with 50 layers per wall are produced in the laboratory environment (Figure 2a, b). The diameter of the AlMg4.5 wire is 1.2 mm. The welding speed was fixed to 0.6 m/min. As a welding program, the Cold Metal Transfer Mix [26] was used with a wire feed rate of 8 m/min and a contact tube to workpiece distance of 12 mm. The produced walls have a length of 150 mm. All the walls are welded either by randomly changing the shielding gas (*Argon 4.6*) flow rate in each layer or by randomly applying oil (with a brush) to the surfaces of the layer before. This approach of randomizing the layers with different shielding gas flow rate and applying oil was taken to ensure the creation of a realistic welding scenario. When oil was applied to the surface of the layer before, the next layer is always welded with a shielding gas flow rate of 15.0 l/min. A weld seam with a shielding gas flow rate of 15.0 l/min without oil is considered to result in good quality weld seams, while one with a lower shielding gas flow rate of 13.5 l/min, 12.0 l/min, 10.5 l/min, and 7.5 l/min or oil was considered to produce imperfection in the weld seam. This assumption was made based on expert reviews and industry norms.

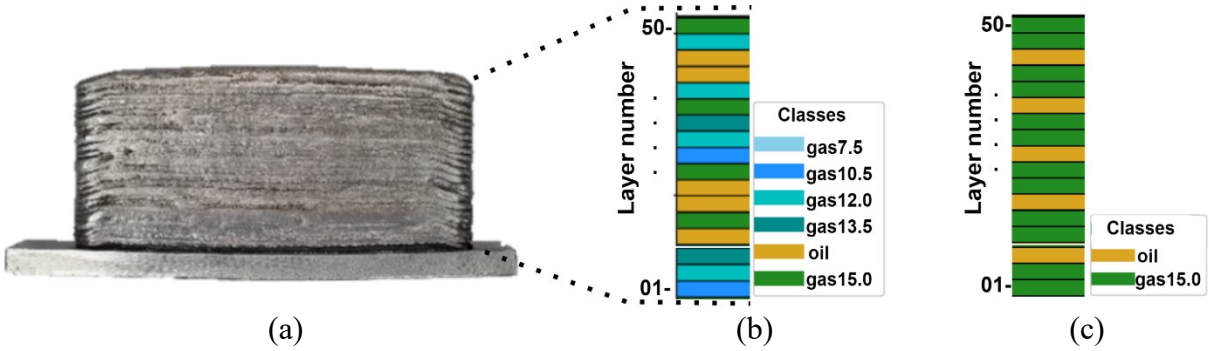

Figure 2. Illustration of DED-Arc based additive manufactured Al wall structure (a) and layer pattern for the Al (b) and for steel (c)

To study the impact of the change in shielding gas flow rate and application of oil in steel material, we further generated 6 walls of steel weld with 50 layers in each wall. The steel structures were constructed using a 1.2 mm diameter steel electrode (1.4430), building up layer by layer. The welding process employed the Cold Metal Transfer Mix with a wire feed rate of 5.2 m/min and a contact tube to workpiece distance of 14 mm. The welding speed was adjusted to 0.4 m/min. A mixture of *Argon* with 18% of CO_2 is used as shielding gas. The steel weld pattern is different from the Al weld experiments (see Figure 2c). This approach was adapted to prevent the potential impact on the layer welded with a shielding gas flow rate of 15.0 l/min and without any oil due to the layer welded before by reduced shielding gas flow rate or the application of oil.

The duration of each audio file is 15 seconds for the Al samples, while for the steel samples, each file is 22 seconds long. In all welding experiments (both Al and steel), welding parameters such as weld speed, current, voltage, and direction of welding are kept constant. Parameters such as welding sessions, amount of oil applied, layer pattern in case of Al structures, environmental conditions, and background sounds are variable.

3. DATASET PROPERTIES

Using the recording configuration described in the previous section, a required dataset was generated for Al and steel material. The scope of this study is focused on the frequency range within the limits of human hearing, which spans up to 20 kHz. Hence, the data recorded with audible range microphone MK202 is considered, and the remaining data is out of scope. Based on the expert review, the small changes in shielding gas flow rate between the neighboring gas classes were insufficient to discern any distinct trends within the data samples. As a result, a decision was made to exclude all intermediate gas classes from further analysis and instead focused exclusively on the highest (15.0 l/min) and lowest (7.5 l/min) shielding gas flow rate classes, in addition to the *Oil* class. By narrowing our focus to these specific classes, we aimed to capture the most significant variations in the data.

The labelling scheme for the welded layers in both Al and steel walls is as follows: Layers welded with 15.0 l/min shielding gas and no oil was labelled as *GasMax*. Layers welded with 15.0 l/min shielding gas and oil were labelled as *Oil*. Layers welded with 7.5 l/min shielding gas and no oil were labelled as *GasMin*. In the case of steel welds, a total of three walls (50 layers per wall) welded with specific layer arrangements were considered for this study. The first wall consisted of 50 consecutive *GasMax* layers. The second wall followed a pattern where two consecutive *GasMax* layers were followed by one *GasMin* layer. This pattern repeated throughout the wall. The third wall featured a pattern where two consecutive *GasMax* layers were followed by one *Oil* layer. This pattern was repeated until the 50th layer. In the case of

consecutive *GasMax* layers, we only consider the top layer as there is a possibility that the bottom *GasMax* layer gets influenced by either of the bottom non-*GasMax* layer and the base plate. This further decreases the count of *GasMax* layers. The corresponding number of files (audio recordings from each layer of the wall) per class for both Al and steel materials is shown in Figure 3. This is evident from the file count that both the Al and steel datasets are highly imbalanced.

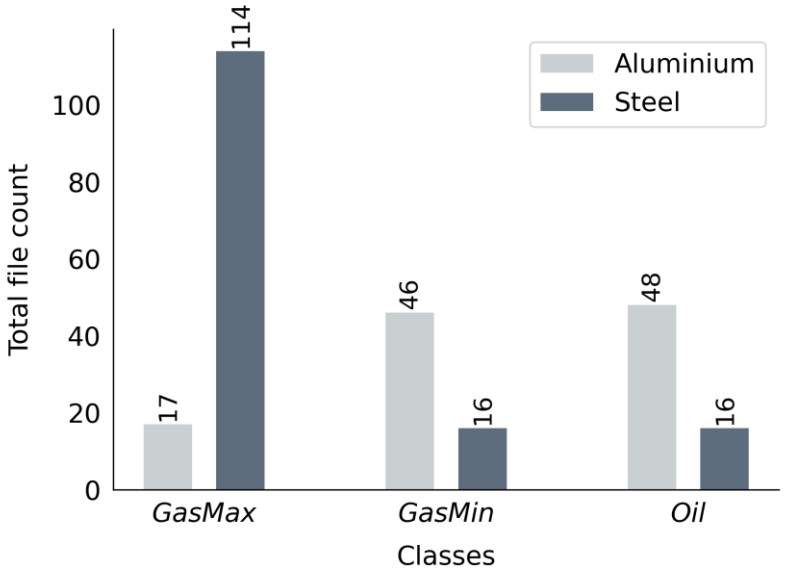

Figure 3. Number of audio files per class in the dataset for steel and Al materials (captured with the MK202 microphone)

4. EXPLORATIVE DATA ANALYSIS

An explorative data analysis (EDA) was performed on recorded audio signals to compare welding irregularities with standard (*GasMax*) class of shielding gas flow rate. To examine the unique patterns of the measured signals in time, frequency and amplitude, a short time fourier transformation method was applied to compute the amplitude spectrogram. In the amplitude spectrograms of the signals, a periodic pulse train was observed along the time axis. These pulses are inherent to the welding process. It is important to note that the amplitude spectrogram could not reveal any strong distinctive information between the standard and other welding irregularity classes. Nevertheless, smaller variations in signal amplitudes were observed, which lead us to further analysis of the root mean square (RMS) level distribution within and between data classes.

To understand the data distribution and the average signal strength within each class, we computed the RMS of the acoustic signals. The process for calculating the RMS value of a signal involves several steps. Firstly, each sample in the signal is squared. Next, the squared samples are averaged by computing the arithmetic mean of all the samples. Lastly, the square root of this average is obtained, resulting in the RMS value of the signal. Furthermore, the RMS values were transformed to the decibel scale (RMS level) to provide a more understandable representation. As a next step, these RMS levels are plotted class-wise with the help of the *violin* plot as shown in Figure 4.

As observed in the case of Al metal welds (Figure 4a), violin for all three classes shows nearly the same RMS level range indicating a stable recording process. The *GasMax* class shows two wide regions (along vertical axis) with different data distributions indicating the difference in the RMS level of the recordings from the different sessions. Similarly, in the case of steel welds (Figure 4b), *GasMax* and *GasMin* classes also show relatively two wide regions

indicating that there were two different data distributions for samples recorded at different sessions. The median of the RMS level (white dot in the centre of violin plot whisker) value for all classes has nearly the same value in the Al and steel datasets. No other substantial deviations were detected in relation to the process parameters, indicating consistent recording conditions. No differences were observed between the three classes based on the RMS level.

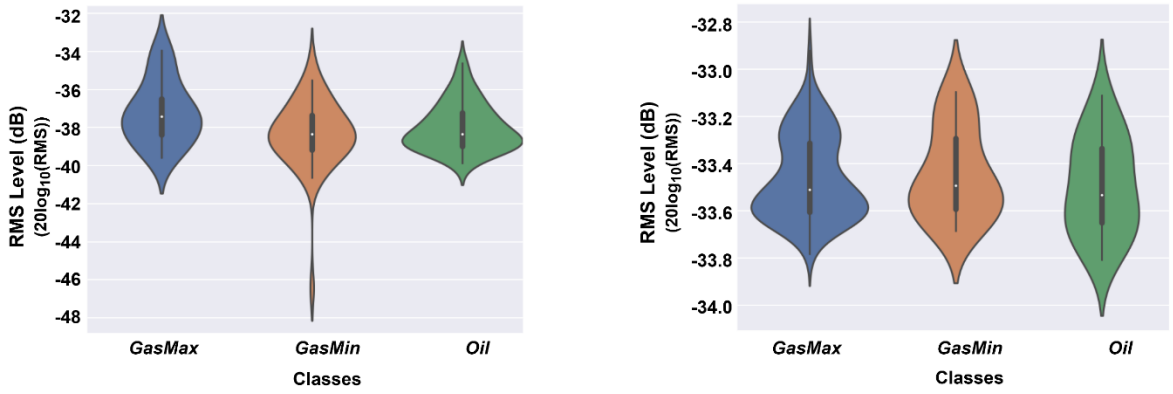

Figure 4. Violin plot showing the RMS level(dB) and data distribution for each of the three weld layer classes for Al (a), and steel (b) material (recordings for MK202 microphone)

To get a deeper look into the data distribution and to examine the correlation among the audio recordings from various classes in the Al and steel datasets, Principal Component Analysis (PCA) [27] was performed.

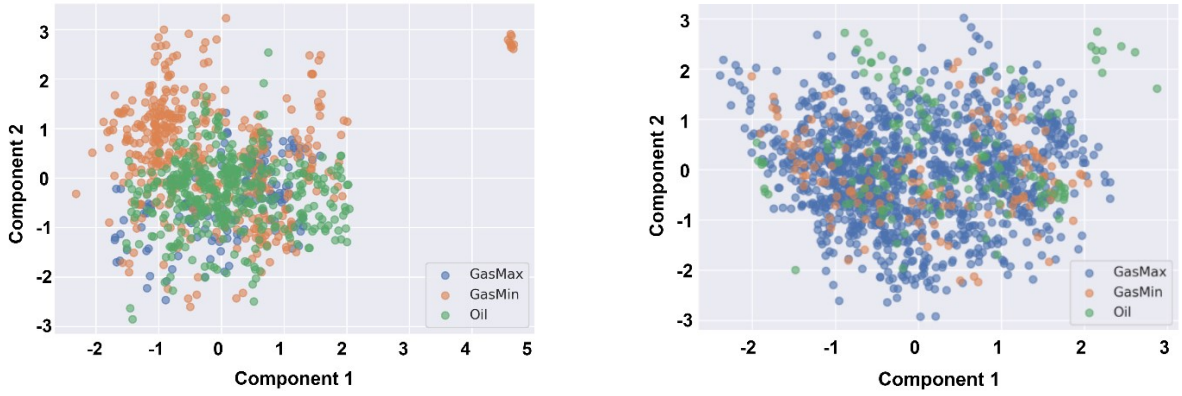

Figure 5. PCA plot for the data samples from the Al (a) and steel (b) wildings with log Mel Spectrogram feature (recordings for MK202 microphone)

In the beginning, PCA was applied on conventional features. These conventional features were calculated by combining metrics like 'RMS', Spectral roll-off, Spectral bandwidth, and others. No significant clustering pattern was observed among the classes. The Mel spectrogram is a time-frequency representation of audio signals that mimic the human auditory system's perception of sound. So, the Mel spectrogram was chosen as the next feature type and performed PCA on them. The features were computed using an FFT size, window size, hop size of 128, 128, 64 samples respectively. The number of Mel bands was set to 16. Further, the features were logarithmically scaled in magnitude to reduce its dynamic range. Each snippet of the audio had a length of 1 second and was separated by a hop of 0.5 seconds.

The PCA plot in Figure 5a show that all three classes exhibit partial overlap with each other indicating shared features or similarities between the classes. No dense cluster is observed in all three classes. Examining the cluster plot further, it becomes evident that all three classes

exhibit low inter-class variance. On the other hand, the intra-class variance is high, implying significant variability within each individual class. Overall, the PCA cluster plot provides insights into the relationships and characteristics of the three classes under investigation.

Further PCA method applied on steel dataset with same feature settings, although no clustering was observed (see Figure 5b). The absence of distinct clusters implies that there is minimal separation between the classes in the reduced-dimensional space. The results indicate that simple linear classifiers are inadequate for the automatic analysis of AE of DED-Arc welding using the GMAW process. Instead, a non-linear classifier is necessary to achieve better detection and classification results. Based on our previous work [28] a non-linear classifier based on neural networks was chosen for further analysis. The classifier is discussed in more detail in the next section.

5. AUTOMATED CLASSIFICATION EXPERIMENTS

As discussed in the welding experiments and AE measurement, experiments were aimed to simulate the standard and the weld seam with irregularities (by varying the shielding gas flow rate and oil contamination). To understand the differences between different welding irregularities that may cause pores in weld seams, EDA was performed on AE data using PCA. However, the results indicated that linear separation was not possible among the considered weld process parameters.

To address this, classification experiments using neural networks were conducted in two tiers. In the first tier, binary classification was performed to detect the difference between the *GasMax* and *GasMin* classes. Subsequently, binary classification was conducted between *GasMax* and *Oil*. Although *GasMax* and *Oil* share the same weld process parameters, the presence of oil contamination could impact the quality of weld seam, which might be reflected in the AE signals. In the second tier, a multiclass classification involving three classes: *GasMax*, *GasMin*, and *Oil* was conducted. This was done to examine how the AE signals differed from the standard process parameters represented by *GasMax*. Both tiers of experiments were conducted using datasets comprising Al and steel welds, separately.

For the detection and classification tasks, a CNN was employed. The subsequent section will discuss the CNN architecture, feature extraction method, and training details.

6. NEURAL NETWORK BASED PIPELINE

Based on the observation, it was noted that the PCA method did not achieve linear separation between classes. Therefore, the decision was made to proceed with utilizing a neural network instead. The log Mel spectrogram was chosen as the preferred input feature type. All the configuration to compute this feature representation remains the same as discussed in previous sections. The input feature representation has a size of 391x16, representing 391 timeframes and 16 Mel bins. To ensure consistency and remove potential transient effects, the first 1 second of each audio recording was discarded before computing the input features.

Next, the architecture of the CNN network used for the detection and classification of the weld parameters is shown in Figure 6. Here, the input data is augmented with Gaussian noise [29] (standard deviation of 0.001) to enhance generalization. L2 regularization (with a coefficient of 0.035) is applied to the weights to prevent overfitting. The model architecture begins with a 2D convolutional layer followed by a ReLU activation function, which introduces non-linearity. A max-pooling layer is then employed to reduce the spatial dimensions and capture the most salient features. Subsequently, a dropout layer with a rate of 0.1 is utilized to prevent overfitting. Another 2D convolutional layer with ReLU activation and a subsequent max pooling layer follow this. The output is then flattened and fed into a dropout layer with a

rate of 0.25. A fully connected layer is introduced to learn complex patterns, followed by another dropout layer with a rate of 0.5 to further regularize the model. Finally, a fully connected layer and a Softmax layer are employed for classification purposes, providing the probability distribution over the output classes.

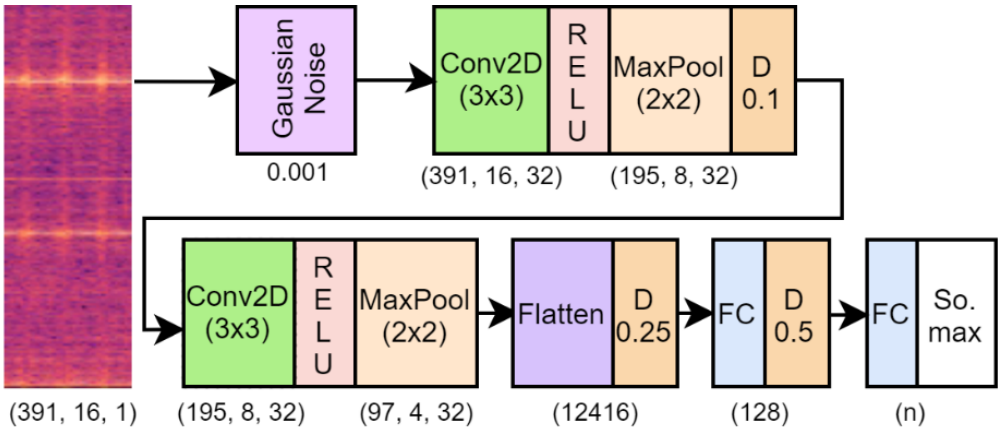

Figure 6. CNN model architecture used for classification of welding irregularities for Al and steel welds. Here, ***n*** *refers to the number of target classes*

Given the smaller size of the Al and steel datasets, the dataset was partitioned into a training and testing set using a 60:40 ratio. This means that 60% of the data was utilized for training the neural network model, while the remaining 40% was reserved for testing its performance. Further, dataset was balanced by applying random oversampling technique. This involves supplementing the training data with multiple copies of the minority classes to match the majority class sample count. A 3-fold cross-validation strategy was employed to ensure robust evaluation of the model's performance. During the training of the model, the categorical cross-entropy loss function is employed: The training process was carried out over 100 epochs. The *Adam optimizer* [30] is a popular choice for training deep neural networks due to its adaptive learning rate and momentum-based updates, which allow for efficient convergence and better generalization. The learning rate of the optimizer is set to 0.001. This combination of data splitting, cross-validation, epoch selection, and optimizer configuration provided a systematic approach to training the neural network model and optimizing its performance on the given dataset. In addition, random erase, SpecAugment and mixup data augmentation techniques were used to tackle the less data problem for the Al and steel weld datasets.

7. RESULTS

The results of the detection and classification experiments discussed in this section are as follows: For the Al dataset, a binary classification conducted between the *GasMax* and *GasMin* classes, achieving a mean accuracy of 82.6% on the test dataset (Figure 7a). Another binary classification was performed between the *GasMax* and *Oil* classes, resulting in a mean accuracy of 65.3% on the test dataset (Figure 7b). Subsequently, a more comprehensive multiclass classification was performed among the *GasMax*, *GasMin*, and *Oil* classes (Figure 7c) resulting in a mean accuracy of 68.1% on the test dataset.

As a result of analyzing the confusion matrices, it was observed that the model tends to misclassify instances from the *GasMax* class as *Oil* class instances, and vice versa. This misclassification could be attributed to the similarity in shielding gas flow rates between the *GasMax* and *Oil* classes. The impact of heat input from the welding arc causes the oil to trickle down the wall, resulting in potential similarities between the AE of these two classes.

Conversely, the *GasMin* class exhibits relatively fewer misclassifications, suggesting a significant difference in emitted sound compared to the other two classes. Furthermore, another possible reason could stem from the data labels, meaning that the welding parameters used to produce irregularities may not consistently result in irregularities during the welding process. This inconsistency in irregularity production may lead to false labels, which could be verified by analyzing the welded structures. By assessing their quality, labels can be corrected.

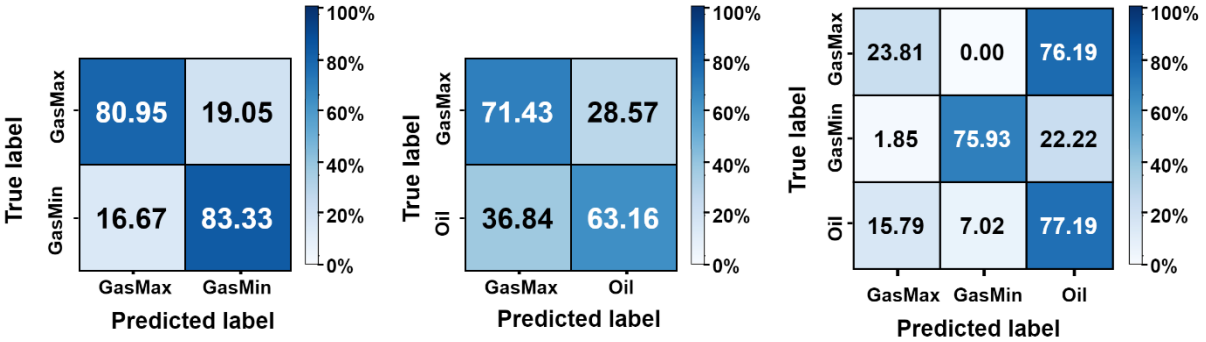

Figure 7. Confusion matrices for GasMax vs GasMin (a), GasMax vs Oil (b), and GasMax vs GasMin vs Oil (c) classification for Al data (results of MK202 microphone)

Regarding steel welds, the model attained a mean accuracy of 81.6% and 85% for binary classification experiments involving *GasMax* vs. *GasMin* (Figure 8a) and *GasMax* vs. *Oil* class (Figure 8b) pairs, respectively.

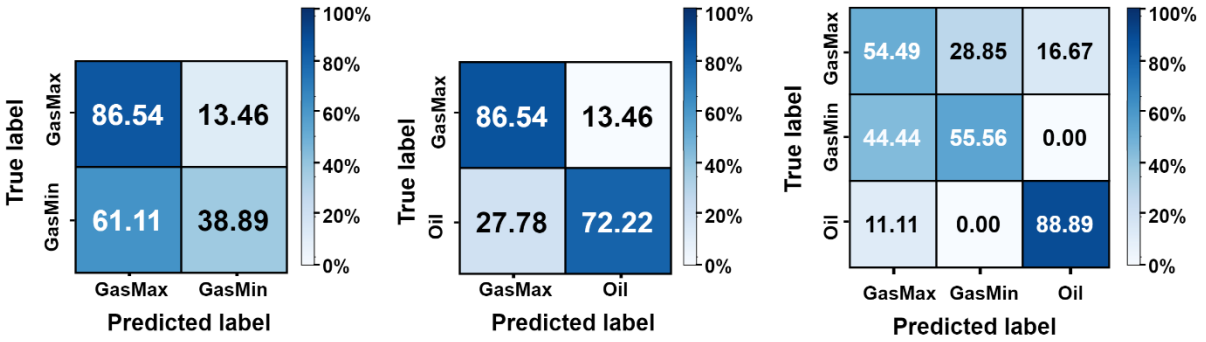

Figure 8. Confusion matrices for GasMax vs GasMin (a), GasMax vs Oil (b), and GasMax vs GasMin vs Oil (c) classification for steel data (results of MK202 microphone)

For the three-class classification experiment (Figure 8c), a mean accuracy of 57.8% is achieved on the test dataset.

It is evident from the confusion matrices that model confuses *GasMin* class with *GasMax* class most of the time. Similar trend was observed with binary and multi-class classification result between the *Oil* and gas classes, where many *Oil* class instances are misclassified as *GasMax* class and never as GasMin class. It is plausible that reduced shielding gas flow rate and oil welding irregularities might not result in significant imperfections in the steel weld seams. The tricking of oil down the steel wall during welding, caused by the heat of the welding arc, could lead to misclassification of the *Oil* as *GasMax* class. This misclassification may occur due to the similar AE characteristics between the *GasMax* and *Oil* classes, given their shared shielding gas flow rate. Further, one valid reason for the poor detection performance of the model for *GasMin* class could be, compared to Al welds, steel welds were not affected by the lack of shielding gas because steel has a higher melting point and is less reactive than Al.

8. CONCLUSION

In this paper, we investigated the potential of using audible range microphones and convolutional neural networks (CNN) to detect and classify weld process irregularities that could potentially lead to the formation of pores in weld seams. We conducted experiments in a controlled laboratory setting, simulating weld process irregularities in aluminum and steel additive manufactured wall structures using the DED-Arc method, which utilizes the GMAW (Gas Metal Arc Welding) technique.

Exploratory data analysis was performed on the aluminum and steel weld datasets. However, linear separability could not be achieved between different weld process parameters. Nevertheless, we found that a non-linear classifier, specifically a CNN trained on log Mel spectrograms, was capable of distinguishing between standard weld process parameter *GasMax* and deviations from standard parameters, such as *Oil* and *GasMin*.

We encountered challenges when classifying oil-contaminated weld seams (represented by the *Oil* class) due to their similarity in process parameters with the *GasMax* class. Consequently, our classifier model misclassified some instances of the *GasMax* as *Oil* class. This highlights the need to examine the physical irregularities in the weld structure when assigning data labels. It is possible that the aforementioned weld irregularities may not always result in the formation of pores, which may not be reflected in the acoustic emissions. Consequently, the models were unable to classify these differences accurately.

In summary, our results demonstrate that weld process irregularities that may lead to imperfection in weld seams can be detected using airborne sound in the audible range. However, further investigation is needed to improve the classification accuracy by considering the physical characteristics of the weld structure for data labeling.

9. ACKNOWLEDGEMENTS

This work has been funded by the Federal Ministry for Education and Research (code 01IS20001E (Projekt AkoS)). The responsibility for the content of this publication lies with the authors.

REFERENCES

[1] Reimann J, Hammer S, Henckell P, Rohe M, Ali Y, Rauch A, Hildebrand J, Bergmann JP. Directed Energy Deposition-Arc (DED-Arc) and Numerical Welding Simulation as a Hybrid Data Source for Future Machine Learning Applications. *Applied Sciences*. 2021 ; 11(15):7075. https://doi.org/10.3390/app11157075

[2] Nadzam, J., et al. "Gas Metal Arc Welding—Product and Procedure Selection." *Lincoln Global Inc.: Cleveland, OH, USA* (2014): C4.

[3] Kodama, S.; Ishida, Y.; Furusako, S.; Saito, M.; Miyazaki, Y.; Nose, T. Arc welding technology for automotive steel sheets. *Nippon Steel Tech. Rep.* **2013**, *103*, 83–90.

[4] Mukai, Y.; Nishimura, A.; Oku, K. CO2 welding of galvanized steel. *Weld. Int.* **1990**, *4*, 123–127.

[5] Oliveira, A.S.; Santos, R.O.d.; Silva, B.C.d.S.; Guarieiro, L.L.N.; Angerhausen, M.; Reisgen, U.; Sampaio, R.R.; Machado, B.A.S.; Droguett, E.L.; Silva, P.H.F.d.; et al. A Detailed Forecast of the Technologies Based on Lifecycle Analysis of GMAW and CMT Welding Processes. *Sustainability* **2021**, *13*, 3766.

[6] Shin, S.; Rhee, S. Porosity characteristics and effect on tensile shear strength of high-strength galvanized steel sheets after the gas metal arc welding process. *Metals* **2018**, *8*, 1077.
[7] Zhang, Z.; Wen, G.; Chen, S. Weld image deep learning-based on-line defects detection using convolutional neural networks for Al alloy in robotic arc welding. *J. Manuf. Process.* **2019**, *45*, 208–216.
[8] Boiler, A. S. M. E., and Pressure Vessel Code. "Section V." *Nondestructive examination* (2010).
[9] Dikbas, H., Caligulu, U., Taskin, M., & Turkmen, M. (2013). X-ray radiography of Ti6Al4V welded by plasma tungsten arc (PTA) welding. *Materials Testing*, *55*(3), 197-202.
[10] Mandache, C., Dubourg, L., Merati, A., & Jahazi, M. (2008). Pulsed eddy current testing of friction stir welds. *Materials Evaluation*, *66*(4).
[11] Hartl R, Bachmann A, Habedank JB, Semm T, Zaeh MF. Process Monitoring in Friction Stir Welding Using Convolutional Neural Networks. *Metals*. 2021; 11(4):535. https://doi.org/10.3390/met11040535
[12] Shin, S.; Jin, C.; Yu, J.; Rhee, S. Real-Time Detection of Weld Defects for Automated Welding Process Base on Deep Neural Network. *Metals* **2020**, *10*, 389. https://doi.org/10.3390/met10030389
[13] Erdmann-Jesnitzer, F., Feustel, E., Rehfeldt, D. (1967). Akustische Untersuchungen am Schweislichtbogen. Schw. und Schn., vol. 19, no. 3, p. 95-100.
[14] Jolly, W.D. (1969). Acoustic emission exposes cracks during welding. Welding Journal, vol. 48, no. 1, p. 21-27.
[15] Rostek, W. (1990). Investigations on the connection between the welding process and airborne noise emission in gas shielded metal arc welding. Schw. und Schn., vol. 42, no. 6, p. E96–E97.
[16] Arata, Y. (1979). Investigation on welding arc sound. Report 1, IIW Doc.S.G.212-451-79.
[17] Horvat, J., Prezelj, J., Polajnar, I., & Čudina, M. (2011). Monitoring Gas Metal Arc Welding Process by Using Audible Sound Signal. *Strojniski Vestnik-journal of Mechanical Engineering, 57*, 267-278.
[18] Mayer, J.L. (1987). Application of acoustic emission to in process monitoring of submerged arc welding. IIW Doc V-WG3- 29-87.
[19] Morita, T., Ogawa, Y., Sumitomo, T. (1995). Analysis of acoustics signals on welding and cutting, Materials Engineering, ASME, vol. III
[20] Ambrosio, D., Dessein, G., Wagner, V., Yahiaoui, M., Paris, J. Y., Fazzini, M., & Cahuc, O. (2022). On the potential applications of acoustic emission in friction stir welding. *Journal of Manufacturing Processes*, *75*, 461-475.
[21] Jolly, W. D. (1969). *USE OF ACOUSTIC EMISSION AS A WELD QUALITY MONITOR* (No. BNWL-SA-2727; CONF-690962-1). Battelle-Northwest, Richland, Wash. Pacific Northwest Lab.
[22] G. K. S. L. Z. Zhong, L. Zheng and Y. Yang, "Random erasing data augmentation," in arXiv, 2017, pp. 1–10.
[23] H. Zhang, M. Cisse, Y. N. Dauphin, & D. Lopez-Paz, "mixup: Beyond empirical risk minimization," in *ICLR* 2018.
[24] Park, D. S., Chan, W., Zhang, Y., Chiu, C. C., Zoph, B., Cubuk, E. D., & Le, Q. V. (2019). Specaugment: A simple data augmentation method for automatic speech recognition. *arXiv preprint arXiv:1904.08779*.
[25] Johnson, D.; Grollmisch, S. Techniques Improving the Robustness of Deep Learning Models for Industrial Sound Analysis. In Proceedings of the 28th European Signal Processing Conference 2020 (EUSIPCO), Virtual Conference, 18–22 January 2021.

[26] Srinivasan, D., Sevvel, P., Solomon, I. J., & Tanushkumaar, P. (2022). A review on Cold Metal Transfer (CMT) technology of welding. Materials Today: Proceedings, 64, 108–115. https://doi.org/10.1016/j.matpr.2022.04.016
[27] Abdi, H., & Williams, L. J. (2010). Principal component analysis. *Wiley interdisciplinary reviews: computational statistics*, *2*(4), 433-459.
[28] S. Grollmisch, et al., “Plastic Material Classification using Neural Network based Audio Signal Analysis,” in *SMSI*, Nürnberg, 2020.
[29] A. Badola, V. P. Nair, and R. P. Lal, "An Analysis of Regularization Methods in Deep Neural Networks," *2020 IEEE 17th India Council International Conference (INDICON)*, New Delhi, India, 2020, pp. 1-6, doi: 10.1109/INDICON49873.2020.9342192.
[30] D. P. Kingma and J. Ba, “Adam: A Method for Stochastic Optimization," in 3rd International Conference on Learning Representations, ICLR 2015, San Diego, CA, USA, May 7-9, 2015, Conference Track Proceedings, Y. Bengio and Y. LeCun, Eds., 2015.

CONTACTS

Jaydeep Chauhan email: jaydeep.chauhan@idmt.fraunhofer.de
ORCID: https://orcid.org/0000-0003-1592-4436
Maximilian Rohe email: maximilian.rohe@tu-ilmenau.de

